Remote Sensing of Environment 115 (2011) 968–977

Contents lists available at ScienceDirect

Remote Sensing of Environment

journal homepage: www.elsevier.com/locate/rse

Improved forest biomass estimates using ALOS AVNIR-2 texture indices

Latifur Rahman Sarker *, Janet E. Nichol

Department of Land Surveying and Geo-Informatics, The Hong Kong Polytechnic University, Hong Kong

ARTICLE INFO

Article history:
Received 18 March 2010
Received in revised form 16 November 2010
Accepted 17 November 2010
Available online 8 January 2011

Keywords:
AVNIR-2
Texture measurement
Biomass estimation
Image processing techniques

ABSTRACT

Optical remote sensing is still one of the most attractive choices for obtaining biomass information, as new sensors are available with fine spatial and spectral resolutions. Better biomass estimates may be possible if suitable processing techniques for these sensors can be demonstrated. This research investigates the potential of high resolution optical data from the ALOS AVNIR-2 sensor for biomass estimation in a mountainous, subtropical forested region using four different types of image processing techniques including i) spectral reflectance and simple spectral band ratio, ii) commonly used vegetation indices, iii) texture parameters and iv) ratio of texture parameters. Simple linear and stepwise multiple regression models were developed between biomass data from 50 field plots, and image parameters derived from these techniques.

Results indicate that spectral reflectance, the simple band ratio, and commonly used vegetation indices have relatively low potential for biomass estimation, as only about 58% of the variability in the field data was explained by the model (adjusted $r^2 = 0.58$ and RMSE = 64 t/ha). However, the texture parameters of spectral bands were found to be effective for biomass estimation with an explained variability of ca. 76% (adjusted $r^2 = 0.76$ and RMSE = 46 t/ha). The result was further improved to adjusted $r^2 = 0.88$ (RMSE = 32 t/ha) using the simple ratio of texture parameters. The results suggest that the performance of biomass estimation can be improved significantly using the texture parameters of high resolution optical data, and further improvement can be obtained using the ratio of texture parameters, as this combines the advantages of both texture and ratio.

1. Introduction

Accurate estimation of forest biomass is required for many purposes especially terrestrial carbon accounting and climate change modeling studies (Brown, 1993; Crow, 1978; Skole et al., 1994). For this, remote sensing techniques are considered necessary because traditional field methods are time-consuming, costly, difficult to implement in remote areas, and only limited to small areas (Hyde et al., 2007). A number of studies have evaluated remote sensing techniques for mapping of forests and forest stand parameters, including height, age, density, biomass and leaf area index, using optical (Boyd et al., 1999; Foody et al., 2001, 2003; Fuchs et al., 2009; Lu, 2005; Muukkonen & Heiskanen, 2007; Steininger, 2000; Thenkabail et al., 2004; Wolter et al., 2009), SAR (Dobson et al., 1992; Foody et al., 1997; Kuplich et al., 2005; Le Toan et al., 1992; Mitchard et al., 2009), LiDAR (Bortolot & Wynne, 2005; Nelson et al., 1988; Patenaude et al., 2004) and multisensor systems (Hyde et al., 2007; Hudak et al., 2002). Although a wide range of approaches has been tested for quantifying biomass, no research has so far demonstrated an operational technique that is consistently accurate and reproducible for quantifying carbon sources and sinks at regional or continental scales (Rosenqvist et al., 2003) because environmental, topographic and biophysical characteristics of forest ecosystems differ in time and space.

In optical remote sensing of biomass, the most widely used procedure is the vegetation index (Foody et al., 2003). Most indices depend on the relationship between red and near-infrared wavelengths to enhance the spectral contribution from green vegetation while minimizing contributions from the soil background, sun angle, sensor view angle, senesced vegetation and the atmosphere (Huete et al., 1985; Karnieli et al., 2001; Tucker, 1979). However, vegetation indices have achieved only moderate success in tropical and subtropical regions where biomass levels are high, the forest canopy is closed, with multiple layering, and there is great diversity of species (Foody et al., 2001; Lu, 2005; Nelson et al., 2000).

Image texture is an important property which can be used to identify objects or regions of interest in an image (Haralick et al., 1973), since it can maximize the discrimination of spatial information independently of tone, thereby potentially increasing the range of biomass to higher levels (Kuplich et al., 2005; Luckman et al., 1997). Many texture measures have been developed based on the grey level co-occurrence matrix (Haralick et al., 1973), texture feature spectrum (He & Wang, 1991), sum and difference histogram (Unser, 1986), variogram (Curran, 1988; Woodcock et al., 1988), and wavelet transform (Laine & Fan, 1993; Luettgen et al., 1993; Unser, 1995), and these have enabled improvements in land use/land cover mapping from both optical and SAR images (Dekker, 2003; Franklin et al., 2000;

* Corresponding author.
E-mail address: lrsarker@yahoo.com (L.R. Sarker).

0034-4257/$ – see front matter © 2010 Elsevier Inc. All rights reserved.
doi:10.1016/j.rse.2010.11.010

Marceau et al., 1990; Podest & Saatchi, 2002; Ryherd & Woodcock, 1996). Moreover image texture has proved to be capable of identifying different aspects of forest stand structure, including age, density and leaf area index (Champion et al., 2008; Cohen & Spies, 1992; St-Onge & Cavayas, 1997; Wulder et al., 1996).

Promising results have been demonstrated using texture measurement for biomass estimation using both optical (Fuchs et al., 2009; Lu, 2005) and SAR data (Champion et al., 2008; Kuplich et al., 2005; Luckman et al., 1997). However, there are some potential problems in implementing texture measurement for biomass estimation, including i) texture is a very complex property and can vary widely depending on the object of interest, physiographic conditions, and the selection of window size (Chen et al., 2004; Franklin, 2001; Franklin et al., 1996; Marceau et al., 1990), ii) texture processing can generate a large amount of data which are difficult to manage (Chen et al., 2004; Franklin, 2001), and there is no indication which texture variables or combination of variables hold the greatest potential and iii) texture measurement is expected to be more effective with higher spatial resolution imagery since finer structural details can be distinguished (Boyd & Danson, 2005; Hay et al., 1996; Hudak & Wessman, 1998; Tuominen & Pekkarinen, 2005). However, most previous biomass estimation projects used Landsat TM data with a 30 m spatial resolution (Lu, 2006). Thus, although texture measurement holds potential for biomass estimation it has not yet been fully investigated and results so far, when applying texture to optical images, have not exceeded 65% of model accuracy, even in structurally simple temperate and boreal forests (Fuchs et al., 2009; Lu, 2005).

This research investigates the potential of the ALOS ANVIR-2 sensor for biomass estimation in a complex sub-tropical forest. This sensor was selected because ANVIR-2 has a 10 m resolution which can give better texture information, and its spectral bands are similar to the first 4 bands of Landsat TM, the most frequently used sensor for biomass estimation so far. The research develops a comparative model by using several image processing techniques including spectral reflectance, simple band ratio, selected vegetation indices and texture processing.

2. Objective

The main objective of this research is to investigate whether texture parameters of AVNIR-2 data are more effective for biomass estimation than spectral information alone, and whether they can solve the saturation problem in high biomass situations.

3. Study area and data

3.1. study area

The study area for this research is the Hong Kong Special Administrative Region (Fig. 1) which lies on the southeast coast of China, just south of the Tropic of Cancer. The total land area of Hong Kong is 1100 km^2 which includes 235 small outlying islands. Although the population is over 7 million, only about 15% of the territory is built-up but less than 1% is still actively cultivated. Approximately 40% of the total area is designated as Country Parks which are reserved for forest succession under the management of the Agriculture, Fisheries and Conservation Department (AFCD). The native sub-tropical evergreen broad leaf forest has been replaced by a complex patchwork of regenerating secondary forest in various stages of development, and plantations. Forest grades into woodland, shrubland then grassland at higher elevations.

3.2. Data

An image collected on 2007-10-24 from the Advanced Visible and Near Infrared Radiometer type 2 (AVNIR-2) of the ALOS was used in this study. The image data have 10 m spatial resolution and comprise four visible wavebands corresponding to blue (0.42 to 0.50 μm), green (0.52 to 0.60 μm), red (0.61 to 0.69 μm) and near infra-red (0.76 to 0.89 μm).

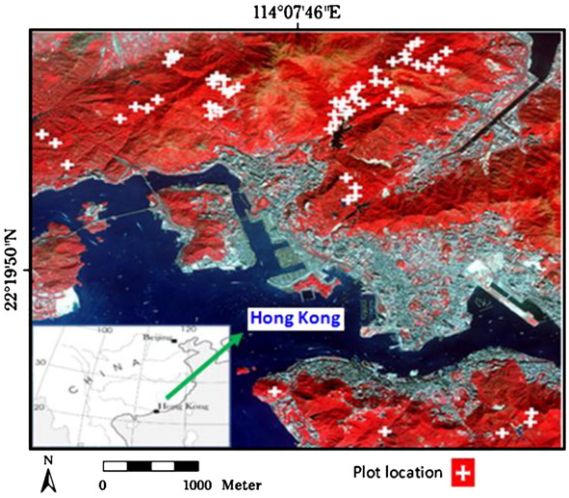

Fig. 1. Study area and location of sample plots.

4. Methodology

The methodology (Fig. 2) of this study comprises two parts i.e. allometric model development for field biomass estimation, and AVNIR-2 image processing. The allometric model was developed based on harvesting of 75 sample trees, and plot biomass data was obtained from field measurement (DBH and height) of 50 sample plots. Image parameters from spectral reflectance, simple band ratio, vegetation indices, texture parameters and the ratio of texture parameters were extracted from all field plots using an area of interest mask (AOI) of 3×3 pixels. In order to explore the potential of different image parameters for biomass estimation, the field plot data were used as the dependent variable and image parameters as independent variables in simple and multiple regression models.

4.1. Allometric model development

An allometric model of the relationship between dry weight (biomass) and an easily measured field parameter was not available. This was developed by harvesting 75 trees (from 14 dominant species) in 4 DBH classes (less than 10, 10–15, 15–20 and above 20 cm), and standard procedures were followed for tree harvesting (Brown et al., 1989; Ketterings et al., 2001; Overman et al., 1994). The measurements of DBH, height and dry weight (DW) were taken for all harvested trees, and regression models used by previous researchers (Arevalo et al., 2006; Brown et al., 1989; Overman et al., 1994) were tested in order to find the best fit using DW as the dependent variable and DBH and height as independent variables in different combinations.

Finally, the best fit model was found using the log transformed DBH and dry weight (DW) as dependent and independent variables respectively in the least square regression model ($\ln DW = a + b*\ln DBH$) because without log transform, the data exhibits heteroscedasticity (i.e. the error variance is not constant across all observations) (Brown et al., 1989; Montagu et al., 2005; Overman et al., 1994). The regression models using logarithmic transforms of variables are usually back-transformed to the power ($\widehat{DW} = e^a . DBH^b$) model and then may be used to predict values of *DW*, given *DBH* in the model. However, inherent in this back-transformed process is a bias that detracts from the accuracy of associated predictors because the anti-log of *In* $\widehat{DW}_i$ is not an unbiased estimate of $\widehat{DW}_i$ i.e.

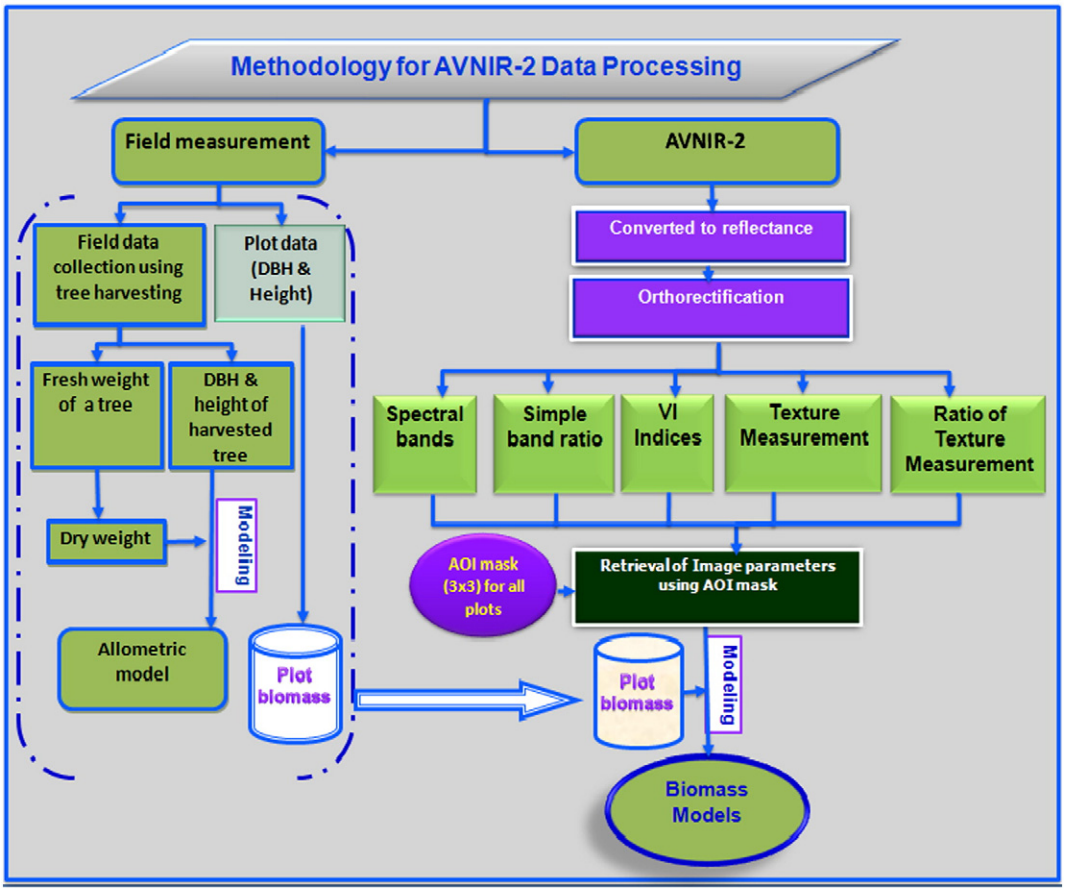

Fig. 2. Overall methodology.

$\widehat{DW}_i \neq e^{\ln \hat{DW}_i}$ (Curtis, 2008). This bias was corrected by multiplying the correction factor (CF) "exp (mse/2 or $S_\varepsilon^2/2$)" according to Baskerville's (1972) multiplicative correction method and the final model was reported in Table 1. The model was tested considering the adjusted r^2, fit index (FI), RMSE and p-level. The FI and RMSE were computed using the data back-transformed from the logarithmic function to real units (Parresol, 1999). The adjusted r^2 (0.93), FI (0.90), and RMSE (13 kg) of the best fit allometric model was highly satisfactory in view of the great variety of tree species, and is similar to the results of several other specialist forest inventories (Brown et al., 1989; Overman et al., 1994).

4.2. Field plot measurement and field biomass estimation

The forest area of Hong Kong is mostly inaccessible, since topographic conditions are very rugged. Due to inaccessibility, random or stratified sampling could not be used for field plot selection. Therefore, after field investigation and consultation with AFCD, purposive sampling was conducted, using 50 field plots to cover a variety of tree stands (from low to high biomass). Circular plots with a 15 m radius were determined considering the image resolution (approximately 10 m), orthorectification error and GPS positioning error. All sample plots were positioned within a homogenous area of forest and at least 15 m distant from other features such as roads, water-bodies and other infrastructure. A Leica GS5+ GPS was used to determine the center of each plot. Measurements were taken using the DGPS mode, with the PDOP value less than 4, to get precise positions. Both DBH and tree height were measured for all trees within the circular plot. Tree DBH was measured at 1.3 m above ground and the heights of small and large trees were measured by Telescopic-5 and DIST pro4 respectively. Trees with DBH below 2.5 cm were not included but were recorded. Finally using the measured parameter DBH, the biomass of each tree and biomass of all trees in a plot were estimated (Table 2) using the allometric model developed for this study area. The biomass of an individual tree in a plot was measured in kilograms (kg). After getting the total weight of all trees in a plot, the biomass density of a plot was measured in metric tons per hectare (t/ha) (Table 2).

4.3. AVNIR data pre-processing

The digital number (DN) of AVNIR-2 data was converted to Spectral Radiance and subsequently to TOA Reflectance. Orthorectification of AVNIR-2 data was carried out using the Satellite Orbital Math Model of PCI Geomatica software (PCI Geomatica, 2007). In order to ensure RMS error within 0.5 pixel, a high resolution (10 m)

Table 1
The best fit allometric model.

Regression model	Coefficient & value		Std err. of coef.	CF (mse/2)	r^2_{adj}	Fit index (FI)	RMSE (kg)	p
$\widehat{DW} = e^a DBH^b e^{mse/2}$	a	−2.057	0.183	0.021	0.93	0.90	13	0.0005
	b	2.289	0.072					

Table 2
Dry weight (biomass) distribution of selected field plots.

Biomass range (t/ha)	Biomass of each plots	Number of plots	Percentage of plots
50–100	50.52, 57.45, 57.53, 61.14, 77.46, 78.11, 82.38, 83.24, 83.87, 92.16, 93.46, 94.68	12	24
100–150	104.60, 106.56, 107.04, 108.10, 109.39, 110.98, 111.67, 120.36, 122.96, 124.13, 131.55, 132.64, 133.07, 136.20, 138.04, 141.90, 147.49, 149.64	18	36
150–200	150.18, 151.46, 156.69, 157.44, 157.59, 163.14, 166.56, 168.02, 177.49, 178.49, 178.89, 188.62, 189.35	13	26
200 & above	270.87, 312.05, 317.93, 346.09, 360.84, 518.60, 530.00	7	14
Total		50	100

DEM, a SPOT-5 image (as reference image), and 76 well distributed GCPs were used. The RMS error in X and Y was 0.29 and 0.25 and the overall error was 0.38 pixel. All images were resampled to a 10 m pixel size using nearest neighbor resampling. Atmospheric correction was carried out using the 6 S atmospheric correction model, with optical depth information from the AERONET station of The Hong Kong Polytechnic University.

4.4. Simple reflectance and band ratio

In addition to the simple reflectance of all four bands (blue, green, red and NIR) of AVNIR-2, six simple spectral band ratios (blue/green, blue/red, blue/NIR, green/red, green/NIR, and red/NIR) were computed in order to investigate the potential for biomass estimation.

4.5. Vegetation indices

A vegetation index simply expresses the image values observed in two or more wavebands as a single value that is related to the biophysical variable of interest (Mather, 1999). Vegetation indices have been recommended for the removal of variability caused by canopy geometry, soil background, illumination angles and atmospheric conditions when estimating biophysical properties such as biomass, Leaf Area Index (LAI) and percent green vegetation cover (Boegh et al., 2002; Curran, 1983; Elvidge & Chen 1995; Schowengerdt, 1983; Tucker, 1979). Their application to tropical forests has been less successful than in other forests (Foody et al., 2001; Lu, 2005; Sader et al., 1989). The reasons for this have been widely discussed from different perspectives (Foody et al., 2001; Le Toan et al., 1992; Moran et al., 1994; Sader et al., 1989; Steininger, 2000; Thenkabail, et al., 2000), and can be summarized as follows;

a) Vegetation indices are mainly successfull for biomass estimation in simply structured temperate and boreal regions (Fassnacht et al., 1997; Fuchs et al., 2009; Peterson et al., 1987; Zheng et al., 2004).
b) In a closed canopy forest, distance-based indices which measure the distance from the soil line (Jackson & Huete, 1991) are irrelevant since the substrate does not contribute to reflectance.
c) Slope-based indices (Jackson & Huete, 1991) which depend on the differential reflectance across the red edge (Tucker, 1979) between red and NIR wavebands, become saturated in complex forests with multiple canopy layers. This is because, although more canopy layers should be related to higher biomass, the ratio is mainly sensitive to the top layer. Thus the relationship between the vegetation index and biomass is asymptotic (Foody et al., 2001) especially in tropical forests with high biomass.
d) In tall complex forests, shadow comprises a larger portion of the tree canopy than in simpler forests for which many vegetation indices were developed, and large areas of low reflectance from shadow areas are not necessarily associated with low biomass.
e) Although many types of vegetation indices can be formed, they cannot be used together as independent predictor variables in multiple regression equations because they are often highly correlated with each other (Foody et al., 2001).

However, despite this allegedly lower performance of vegetation indices in tropical and sub-tropical forest, some commonly used vegetation indices were selected (Table 3) in order to test the performance of the AVNIR-2 sensor and to compare the performance with other processing steps.

4.6. Texture analysis

Texture is a characteristic used to identify objects or regions of interest in any image (Haralick et al. 1973). It is defined as the spatial variability in image tone giving rise to different neighboring pixel values for the same apparent target type (Luckman et al., 1997). Indeed, in high resolution images, texture, not intensity, is usually the most important source of information (e.g., Dell'Acqua & Gamba, 2003; Podest & Saatchi, 2002; Ulaby et al., 1986). Among the several texture algorithms two categories of texture measurement were selected, to test their potential for biomass estimation with AVNIR-2 data (Table 4) as these are basic, widely used and simple algorithms. The first is the grey level co-occurrence matrix (GLCM) (Haralick

Table 3
Selected vegetation indices used for biomass estimation.

Slope-base vegetation indices		Distance-based vegetation indices	
Vegetation index	References	Vegetation index	References
Infrared/visible ratio	Gibson and Power (2000)	Perpendicular vegetation index 1 (PVI1)	Perry and Lautenschlager (1984)
Reflectance ratio or ratio vegetation index (RVI)	Pearson and Miller (1972)	Perpendicular vegetation index 2 (PVI2)	Bannari et al. (1996)
Normalized difference vegetation index (NDVI)	Rouse et al., 1974; Kriegler et al., 1969	Perpendicular vegetation index 3 (PVI3)	Qi et al. (1994)
Transformed vegetation index (TVI)	Deering et al. (1975)	Difference vegetation index (DVI)	Richardson and Wiegand (1977)
Corrected transformed vegetation index (CTVI)	Perry and Lautenschlager (1984)	Soil-adjusted vegetation index (SAVI)	Huete (1988)
Thiam's Transformed Vegetation Index (TTVI)	Thiam (1997)	Transformed Soil-adjusted Vegetation Index (TSAVI 1)	Baret et al. (1989)
Normalized ratio vegetation indexes (NRVI)	Baret and Guyot (1991)	Modified soil-adjusted vegetation index 1 (MSAVI1)	Qi et al. (1994)
Modified simple ratio (MSR)	Chen (1996)	Modified soil-adjusted vegetation index 2 (MSAVI2)	Qi et al. (1994)
Infrared percentage vegetation index (IPVI)	Crippen (1990)	Weighted difference vegetation index (WDVI)	Richardson and Wiegand, 1977; Clevers, 1988
Perpendicular vegetation index (PVI)	Richardson and Wiegand (1977)	Global environment monitoring index (GEMI)	Pinty and Verstraete (1991)
		Soil and atmospherically resistant vegetation index (SARVI)	Kaufman and Tanre (1992)

Table 4
The formula of texture measurements used in this study.

Grey level co-occurrence matrix (GLCM) based texture parameter estimation	Sum and difference histogram (SADH) based texture parameter
1. $Mean(ME) = \sum_{i,j=0}^{N-1} iP_{i,j}$	1. $Mean(\mu) = \frac{\sum_{i,j} x_{ij}}{n}$
2. $Homogeneity(HO) = \sum_{i,j=0}^{N-1} i \frac{P_{ij}}{1+(i-j)^2}$	2. $Mean\ deviation(MD) = \frac{\sum_{i,j} x_{ij}-\mu}{n}$
3. $Contrast(CO) = \sum_{i,j=0}^{N-1} iP_{i,j}(i-j)^2$	3. $Mean\ Euclidean\ distance(MED) = \sqrt{\frac{\sum_{i,j}(x_{ij}-x_c)^2}{n-1}}$
4. $Standard\ deviation(Std) = \sqrt{VA}$	4. $Variance(\sigma^2) = \frac{\sum_{i,j}(x_{ij}-\mu)^2}{n-1}$
where $VA = = \sum_{i,j=0}^{N-1} iP_{ij}(i-ME)^2$	
5. $Dissimilarity(DI) = \sum_{i,j=0}^{N-1} iP_{i,j}\lvert i-j\rvert$	5. $Normalized\ Coefficient\ of\ Variation(NCV) = \sqrt{\frac{\sigma^2}{\mu}}$
6. $Entropy(EN) = \sum_{i,j=0}^{N-1} iP_{i,j}(-\ lnP_{i,j})$	6. $Skewness(Sk) = \frac{\sum_{i,j}(x_{ij}-\mu)^3}{(n-1)\sigma^3}$
7. $Angula\ Second\ Moment(ASM) = \sum_{i,j=0}^{N-1} iP_{i,j}^2$	7. $Kurtosis(Ku) = \frac{\sum_{i,j}(x_{ij}-\mu)^4}{(n-1)\sigma^4}$
8. $Inverse\ Difference(ID) = \sum_{i,j=0}^{N-1} i \frac{P_{ij}}{\lvert i-j\rvert 2}$	8. $Energy(E) = \sum_{i,j} x_{ij}^2$
9. $GLDV\ Angular\ Second\ Moment(GASM) = \sum_{k=0}^{N-1} V_k^2$	9. $Entropy(H) = \sum_{i,j} p_{i,j}\ ln(p_{i,j}),\quad with\ p_{ij} = \frac{x_{ij}}{\sum_{i,j} x_{ij}}$
10. $GLDV\ Entropy(GEN) = \sum_{k=0}^{N-1} V_k(-\ lnV_k)$	
Here, P (i, j) is the normalized co-occurrence matrix such that SUM (i, j = 0, N-1) (P (i, j)) = 1. V(k) is the normalized grey level difference vector V(k) = SUM (i, j = 0, N-1 and |i–j| = k) P (i, j)	Here, x_{ij} stands for the pixel value of pixel (i,j) in the kernel over which is summed, n for the number of pixels that is summed, x_c for the kernel's center pixel value, and p_{ij} for the normalized pixel value.

et al., 1973) along with some Grey Level Difference Vector (GLDV)-based texture measurements. The second is the sum and difference histogram proposed by Unser (1986) as an alternative to the usual co-occurrence matrices used. Identifying suitable textures additionally involves the selection of moving window sizes (Chen et al., 2004; Lu, 2005). A small window size exaggerates the difference within the window but retains high spatial resolution, while a large window may not extract texture information efficiently due to over-smoothing of the textural variations. The resolution of the data used is high (10 m), similar to the 8–10 m mean size of tree crowns. Since the forest canopy is closed, this means that portions of tree crowns and shadows may be amalgamated (thus averaged) in some pixels, but remain discrete in others. Since the recurring patch size of the forest, determined mainly by topography, is roughly 100–200 m, we selected small to medium window sizes (9 9 and lower) to operate within those patches. Four detecting directions (0^0, 45^0, 90^0 and 135^0) were specified for the processing.

4.7. Statistical analysis

To represent the relationship between field biomass and remotely sensed data, some researchers have used linear regression models with or without log transformation of field biomass data (Calvao & Palmeirim, 2004; Salvador & Pons, 1998; Steininger, 2000), while others have used multiple regression (Hyde et al., 2006; Zheng, et al., 2004). Non-linear regression (Santos et al., 2003), Artificial Neural Networks (Foody et al., 2001; Kimes et al., 1998) and semi-empirical models (Castel et al., 2002) have also been examined.

Although no model can perfectly express this complex relationship, researchers are still using multiple regression models as one of the best choices. In this research, simple linear regression and stepwise multiple-linear regression models were used to compare data derived from all processing steps with field biomass. Biomass data were collected from 50 field plots and were used as dependent variables. The spectral reflectance of each field plot was extracted using an area of interest (AOI) mask of 3×3 pixels and mean reflectance was calculated.

In multiple regression modeling, difficulties such as multicollinearity and overfitting may arise when a large number of independent variables are used, as these variables maybe highly correlated to one another. To avoid overfitting problems, as well as to ensure finding the best fit model, three common statistical parameters, namely adjusted r^2, RMSE, and p-level (for the model) were computed. Another seven statistical parameters such as Beta coefficient (B), Std. Error of B, p-level, tolerance ($Tol = Tolerance = 1 - R_x^2$), variance inflation factor ($VIF = VIF_j = \frac{1}{1-R_j^2}$), and condition index ($CI = k_j = \frac{\lambda_{max}}{\lambda_j},\ j = 1, 2, \ldots, p$) were calculated to test intercept fitness and multicollinearity effects. To indicate multicollinearity problems, a tolerance value of less than 0.10 (Belsley, 1990), VIF value of greater than 10 (Belsley, 1990; Douglas et al., 2006; Hyde et al., 2007; Kutner et al., 2005), and condition index greater than 30 (Belsley, 1990; Douglas et al., 2006) were used as determinants.

4.8. Processing of AVNIR-2 data for modeling

The AVNIR-2 data were processed in the following four steps:

(i) Spectral reflectance and simple ratio of spectral reflectance were used individually in linear regression, and together in the multiple regression model.
(ii) Image parameters from commonly used vegetation indices were used in linear regression individually and together in a stepwise multiple regression model.
(iii) Texture parameters from each spectral band of AVNIR-2 sensor, and all bands together, were used in a stepwise multiple regression model.
(iv) The ratio of texture parameters of 6 band combinations (1/2, 1/3, 1/4, 2/3, 2/4, and 3/4) were used in a stepwise regression model, both individually and combined.

5. Results and analysis

5.1. Step-1: Performance of raw data processing, simple ratio and vegetation indices

The relationships between field biomass and the spectral signature of AVNIR-2 data were found to be poor for all spectral bands individually, though stronger correlations were observed using band

4 (near infrared) (adjusted $r^2 = 0.48$ and RMSE = 71 t/ha) and band 2 (green) (adjusted $r^2 = 0.13$ and RMSE = 93 t/ha). This only moderate result achieved concurs with many other studies (Foody et al., 2001; Salvador & Pons, 1998; Steininger, 2000; Thenkabail et al., 2004).

Overall the performance of simple band ratio was better than any single spectral band, with highest adjusted r^2 of 0.58 (RMSE = 63 t/ha) obtained using the ratios 3/4 and 1/4. Results for the 10 vegetation indices tested gave a similar result to simple band ratios, with the best results from slope-based indices, which are essentially different combinations of the red and NIR bands. The RVI represented the overall highest variability in the field data (adjusted $r^2 = 0.58$), but others such as the NDVI in 5th place (adjusted $r^2 = 0.57$ and RMSE = 64 t/ha) gave similar performance. This improvement over single bands is attributed to enhancement of the spectral contribution from green vegetation while minimizing contributions from soil background, sun angle, sensor view angle, senesced vegetation and the atmosphere (Huete et al., 1985; Tucker, 1979), in the complex forest structure and high biomass in tropical or subtropical forest discussed above (Section 1).

However, although the 58% variability of the model (adjusted $r^2 = 0.58$ and RMSE = 63 t/ha) obtained here using both simple band ratios and vegetation indices is not as high as the $r^2 = 0.82$ obtained by Zheng et al. (2004) in simply-structured temperate forests, it is considerably higher than previous results in tropical forests (Foody et al., 2001; Lu, 2005; Rahman et al., 2005; Steininger, 2000). For example, using Landsat with 30 m resolution, Foody et al. (2001) found insignificant relationships using 230 permutations of six conventional vegetation indices for tropical forests with high biomass up to 400 t/ha, and Rahman et al. (2005) obtained an r^2 of 0.47.

5.2. Step-3: Performance of texture processing

Texture measurements showed a significant improvement in biomass estimation using ANVIR-2 data. The texture parameters of bands 4 and 3 respectively obtained the best (adjusted $r^2 = 0.72$ and RMSE = 51 t/ha) (model 4 in Table 5) and poorest performance (adjusted $r^2 = 0.31$ and RMSE = 83 t/ha) (model 3 in Table 5). This result for band 4 was much better than for the raw band without texture (adjusted $r^2 = 0.48$ and RMSE = 71 t/ha) (Fig. 3a).

Further improvement was achieved using the texture parameters of all bands together in a multiple regression model (model 5 in Table 5 and Fig. 3a). Approximately 76% of the variability in field biomass (adjusted $r^2 = 0.76$ and RMSE = 46 t/ha) was obtained. Moreover it is important to note that the model, and all variables were significant and multicollinearity effects were not observed. Generally, window sizes 7×7 and 9×9 were more successful, probably due to their greater sensitivity to the inter-pixel differences in the proportions of tree crown and shadow respectively within each pixel (Fuchs et al., 2009; Lu, 2005), as such differences would be averaged out by larger windows (Franklin et al., 2000).

Improvement of biomass estimation using texture parameters of optical data is also noted by Lu (2005) ($r^2 = 0.49$) in tropical forest and Fuchs et al. (2009) ($r^2 = 0.63$) in temperate forest since texture can represent differences in forest stand structure due to its sensitivity to the spatial aspects of canopy shadow. Although we obtained a better model using texture parameters of all bands, with greatly improved performances compared with previous studies in both tropical and temperate forests (ibid), this model can still only explain 76% of the variability in field biomass. Moreover, the RMSE of 46 t/ha is still large because some high biomass plots are still far from the fitted line (Fig. 4a). Therefore since a robust model for biomass estimation had not yet been obtained, the researchers decided to explore further using a simple ratio of texture parameters, in order take advantage of both texture processing and band ratio combined.

5.3. Step-4: Performance of ratio of texture parameters

In general, biomass estimation was improved using the ratio of the texture parameters of individual bands (Table 6). The highest adjusted r^2 of 0.88 (RMSE = 32 t/ha) was obtained from all the texture ratios combined (model 7 in Table 6 and Fig. 3b). This was a

Table 5
Results obtained from texture parameters of ANVIR-2 data.

Data	Model fitting parameters			Fitting parameters for intercept and variables						
	r^2_{adj}	RMSE (t/ha)	p-level	Variables name & intercept	B	Std. Err. of B	p-level	Tol	VIF	CI
Model-1 texture of band-1	0.29	81	0.00	Intercept	646.87	110.70	0.000			
				GASM_W7×7	516.02	151.27	0.001	0.366	2.72	2.47
				HO_W9×9	−975.96	211.13	0.000	0.281	3.55	11.26
				CO_W9×9	−13.71	3.68	0.001	0.656	1.52	29.47
Model-2 texture of band-2	0.50	67	0.00	Intercept	458.35	89.83	0.000			
				Ku_W9×9	11.65	4.23	0.009	0.558	1.79	2.19
				CO_W9×9	−13.18	2.53	0.000	0.515	1.94	3.79
				HO_W9×9	−677.12	182.68	0.001	0.314	3.18	5.41
				Sk_W7×7	51.88	16.75	0.003	0.604	1.65	7.77
				ASM_W9×9	597.29	224.16	0.011	0.301	3.32	29.16
Model-3 texture of band-3	0.28	83	0.00	Intercept	280.84	41.94	0.000			
				EN_W7×7	−148.99	32.54	0.000	0.650	1.53	6.89
				NCV_W3×3	3363.48	1334.89	0.015	0.650	1.53	8.39
Model-4 texture of band-4	0.72	51	0.00	Intercept	150.91	58.98	0.014			
				E_W9×9	−0.001	0.000	0.002	0.582	1.71	1.73
				ASM_W9×9	1630.37	272.76	0.000	0.545	1.83	3.17
				CO_W9×9	14.10	3.01	0.000	0.691	1.44	6.29
				Sk_W5×5	39.39	16.71	0.023	0.617	1.62	17.91
Model-5 texture of all bands	0.76	46	0.00	Intercept	462.67	58.16	0.000			
				ME_W5×5	−13.32	2.47	0.000	0.665	1.50	2.31
				Ku_W9×9	12.46	2.57	0.000	0.728	1.37	3.73
				CO_W9×9	10.37	2.57	0.000	0.823	1.21	4.74
				EN_W9×9	−58.13	15.53	0.001	0.773	1.29	7.04
				Sk_W5×5	51.01	15.81	0.002	0.660	1.51	11.12
				Sk_W9×9	−23.91	10.57	0.029	0.674	1.48	25.58

W = window size.

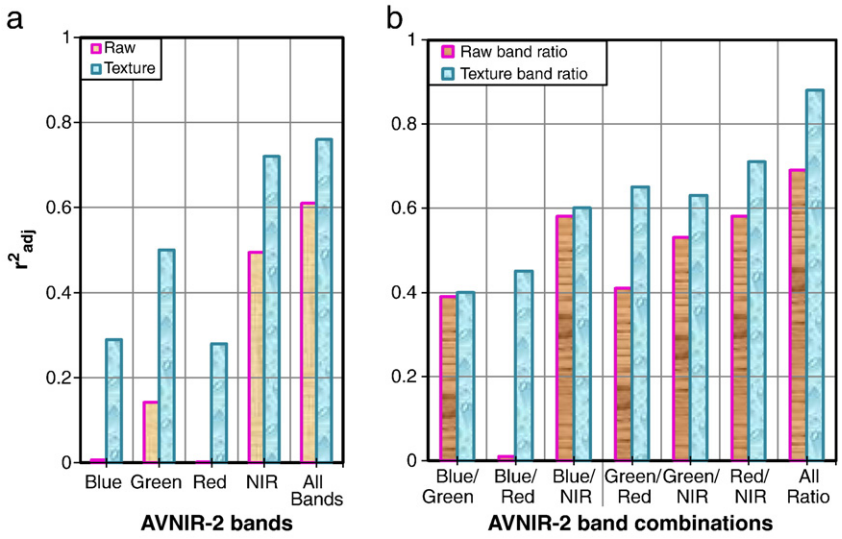

Fig. 3. Comparison of biomass estimation performance a) between spectral bands and texture parameters, and b) between spectral band ratios and texture parameter band ratios.

significant improvement in biomass estimation compared to the best result obtained using raw spectral bands (adjusted $r^2 = 0.48$ and RMSE = 71 t/ha), simple ratio (adjusted $r^2 = 0.58$ and RMSE = 63 t/ha), selected vegetation indices (adjusted $r^2 = 0.58$ and RMSE = 63 t/ha) and texture parameter models (adjusted $r^2 = 0.76$ and RMSE = 46 t/ha). The model and all variables were significant, and multicollinearity effects were not evident. The relationships between the model predicted, and observed biomass also showed a good fit to the regression line (Fig. 4b) except for one high biomass plot far from the line which yielded an RMSE of 32 t/ha. Although this RMSE seems to be large, considering the high biomass range of this study area (from 52 t/ha to 530 t/ha) this error is relatively small.

Comparing the ratio of raw spectral bands with the ratio of the texture bands, we found improved performance in all cases. The highest adjusted r^2 obtained by the raw band ratio (red/NIR or blue/NIR, Fig. 3b) was 0.58 (RMSE = 63 t/ha), while the highest adjusted r^2 of 0.72 (RMSE = 51 t/ha) was obtained from the texture band ratio of red/NIR(Fig. 3b).

6. Discussion

Among the four different data processing techniques applied to investigate the potential of ANVIR-2 data for biomass estimation, the best result (adjusted r^2) obtained from single band spectral reflectance (0.48 from NIR), simple band ratios (0.58 from red/NIR or blue/NIR) and vegetation indices (0.58 from RVI) was not very promising, with a best fit model representing only 58% of the variability in biomass (adjusted $r^2 = 0.58$ and RMSE = 63 t/ha). Considerable improvement was observed using the texture parameters of single bands (adjusted $r^2 = 0.72$ and RMSE = 51 t/ha) and texture parameters of all bands together (adjusted $r^2 = 0.76$ and RMSE = 46 t/ha), and an even higher adjusted r^2 of 0.88 (RMSE = 32 t/ha) was obtained when the simple ratio of texture parameters was used in the model. We attribute this high performance to the processing techniques applied and the high resolution of the data used.

The moderate result achieved using spectral reflectance bands maybe explained by the fact that field biomass levels in this study area are very high and although near infrared reflectance from the spongy mesophyll of a single leaf layer increases initially with increasing leaf cover, as additional leaf layers are added to a canopy these increases are not sustained (Jensen, 2000). Concurrently, as the canopy matures, creating more layers and increasing in complexity, shadowing acts as a spectral trap for incoming energy and reduces the amount of radiation returning to the sensor (Moran et al., 1994).

In this research we tested six combinations of simple spectral band ratios and some commonly used vegetation indices in order to investigate the possibilities of using fewer vegetation indices, as there are many vegetation indices available, but no guidelines as to their potential in different situations. The results indicate that either simple spectral band ratios (such as red/NIR), or complex vegetation indices (such as NDVI or MSAVI or RVI) perform better than single spectral bands, but differences in performance between simple band ratios and complex vegetation indices are not pronounced.

The main indication is that when the canopy is full and forest is continuous then neither slope-based vegetation indices such as NDVI nor distance-based vegetation indices such as PVI, or MSAVI are more useful than simple band ratios: a finding which supports other researchers working in tropical forests (Foody et al., 2001; Lu, 2005). The reasons for this have been widely discussed (Foody et al., 2001; Le Toan et al., 1992; Moran et al., 1994; Sader et al., 1989; Thenkabail et al., 2000), and we have summarized the main points in Section 4.5. The performance of the biomass estimation can be improved using all spectral bands and all vegetation indices together in the model, however, both models violated the assumption of uncorrelated independent variables and resulted in multicollinearity effects (CI more than 30).

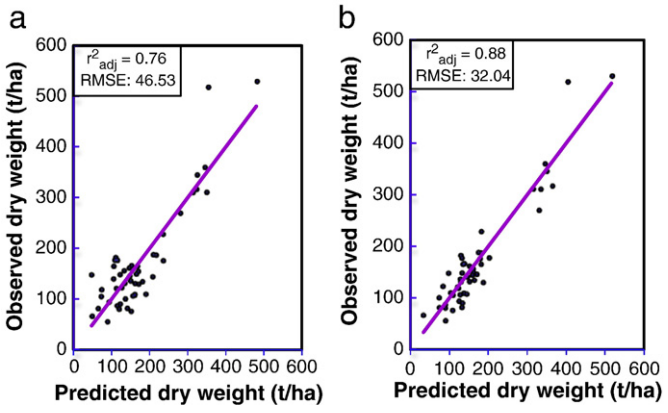

Fig. 4. Relationships between observed and model predicted biomass using a) texture parameters (model-5 in Table 5), and b) ratio of texture parameters (model-7 in Table 6), of AVNIR-2 data.

Table 6
Results obtained from ratio of texture parameters of AVNIR-2 data.

Data	Model fitting parameters			Fitting parameters for intercept and variables						
	r^2_{adj}	RMSE (t/ha)	p-level	Variables name & intercept	B	Std. err. of B	p-level	Tol	VIF	CI
Model-1 texture-ratio (band1/band2)	0.40	76	0.00	Intercept	53.29	23.18	0.026			
				ME_W9×9	82.70	23.44	0.001	0.704	1.42	4.12
				σ^2_W9×9	137.99	67.67	0.047	0.704	1.42	4.61
Model-2 texture-ratio (band1/band3)	0.45	73	0.00	Intercept	67.84	20.59				
				DI_W9×9	395.16	63.165	0.000	0.165	6.05	2.99
				CO_W9×9	−348.72	69.088	0.000	0.165	6.05	9.20
Model-3 texture-ratio (band1/band4)	0.60	63	0.00	Intercept	−61.59	28.81	0.038			
				E_W5×5	927.97	108.72	0.000	1.00	1.00	6.12
Model-4 texture-ratio (band2/band3)	0.65	57	0.00	Intercept	239.26	48.91	0.000			
				ME_W9×9	−379.37	58.09	0.000	0.988	1.01	4.82
				EN_9×9	118.08	20.21	0.000	0.991	1.00	6.58
				μ_W5×5	−45.31	14.01	0.002	0.992	1.00	13.06
Model-5 texture-ratio (band2/band4)	0.63	59	0.00	Intercept	236.36	109.65				
				E_W9×9	2273.17	317.73	0.000	0.874	1.14	3.59
				GEN_W9×9	−334.44	87.36	0.000	0.429	2.32	9.62
				ASM_W9×9	−15.76	5.32	0.005	0.395	2.53	29.42
Model-6 texture-ratio (band3/band4)	0.71	51	0.00	Intercept	77.31	41.71	0.070			
				GEN_W9×9	−187.91	42.93	0.000	0.875	1.14	4.59
				E_W9×9	6309.94	701.77	0.000	0.564	1.77	7.52
				ME_W3×3	−288.68	107.13	0.010	0.543	1.84	12.99
				Ku_W5×5	−26.32	12.01	0.034	0.884	1.13	13.32
Model-7 texture-ratio (all band ratio together)	0.88	32	0.00	Intercept	118.49	39.31	0.004			
				GEN_BR_1/4_W9×9	−112.38	34.47	0.002	0.617	1.62	4.32
				ASM_BR_2/3_W7×7	−84.38	26.61	0.003	0.379	2.63	6.56
				GET_BR_2/3_W7×7	−50.45	15.74	0.003	0.475	2.10	7.91
				DI_BR_2/3_W9×9	107.88	17.26	0.000	0.590	1.69	10.28
				Std_BR_2/4_W5×5	−134.78	27.96	0.000	0.340	2.94	10.93
				ME_BR_2/4_W9×9	−1327.87	102.30	0.000	0.384	2.60	15.33
				ME_BR_3/4_W9×9	1296.57	95.64	0.000	0.240	4.16	20.07
				Ku_BR_2/3_W5×5	58.74	10.68	0.000	0.680	1.47	26.36

W = window size, and BR = band ratio.

Biomass estimation was improved using texture parameters of all spectral bands together in the model, with almost 76% of the variability in field biomass (adjusted $r^2 = 0.76$ and RMSE = 46 t/ha). This significant improvement using texture was not completely unexpected as many researchers (Fuchs et al., 2009; Lu, 2005) have also observed better results using texture measurement with optical data, but considering the very high biomass levels of this study area, this result seems very promising.

We achieved even higher model performance (adjusted $r^2 = 0.88$ and RMSE = 32 t/ha) using the simple ratio of texture parameters, which has not been reported previously for biomass estimation. We know that texture measurements have the potential to improve biomass estimation using optical images, by simplifying the canopy structure (Fuchs et al., 2009; Lu, 2005), and band ratios have the ability to improve biomass estimation compared to a single band, by minimizing contributions from sun angle, sensor view angle, atmospheric condition and canopy geometry (Boegh et al., 2002; Curran, 1983; Elvidge & Chen, 1995; Franklin, 2001; Huete et al., 1985; Schowengerdt, 1983; Tucker, 1979). The ratio of texture parameters, combines both techniques (texture measurement and ratio) to improve biomass estimation and we attribute the observe very significant improvement, to the combination of two well-known processing techniques, namely texture measurement and image ratio together. The good results obtained from this research are also due to the high resolution of the AVNIR-2 compared with previous sensors used for biomass studies, as texture is more capable of defining the forest structure with fine spatial resolution imagery (Boyd & Danson, 2005; Franklin et al., 2000; Hay et al., 1996; Tuominen & Pekkarinen, 2005).

7. Conclusion

The potential of optical imagery for biomass estimation was explored using data from AVNIR-2 sensor and significant improvement was obtained using the ratio of texture indices in a high biomass situation. The ratio of texture indices for biomass estimation has not been investigated previously, but the promising result (adjusted $r^2 = 0.88$) demonstrated here indicates that it has greater potential for biomass estimation than other image processing techniques. This improved performance compared to other studies in tropical regions may be due to several other factors, including i) the higher (10 m) resolution of the AVNIR-2 data, compared to the 30 m resolution of Landsat TM used in most previous studies, ii) the good fit of the allometric model devised for this study, iii) the large size of field plots compared to the image resolution, and accuracy of locating them on the image in our local study area, and iv) the large number of field plots for model development. However, although this work was based on only one study area and some commonly used texture algorithms, we do believe that texture properties will remain important for biomass estimation in most forest conditions using 'high' resolution sensors. Furthermore, since these techniques proved effective in a challenging study area with rugged relief, high species diversity and high biomass, they are likely to be effective for other study areas, although researchers would need to test the different texture algorithms, window sizes, and combinations of parameters in their study context.

Acknowledgements

The authors would like to thank the Hong Kong Agriculture, Fisheries and Conservation Department for their help with the tree harvesting in the country parks and the Japan Aerospace Exploration Agency for the ALOS images, under ALOS agreement no. 376. The authors are also very thankful to the reviewers for their very constructive comments. This work was supported by GRF Grant PolyU5281/09E.

References

Arevalo, C. B. M., Volk, T. A., Bevilacqua, E., & Abrahamson, L. (2006). Development and validation of aboveground biomass estimations for four Salix clones in central New York. *Biomass and Bioenergy*, *31*, 1−12.

Bannari, A., Huete, A. R., Morin, D., & Zagolski (1996). Effets de la Couleur et de la Brilliance du sol sur les Indices ds Vegetation. *International Journal of Remote Sensing*, *17*, 1885−1906.

Baret, F., & Guyot, G. (1991). Potential and Limits of Vegetation Indices for LAI and AFAR Assessment. *Remote Sensing of Environment*, *35*, 161−173.

Baret, F., Guyot, G., & Major, D. (1989). TSAVI: A Vegetation Index Which Minimizes Soil Brightness Effects on LAI and APAR Estimation. *12th Canadian Symposium on Remote Sensing and IGARSS'90, Vancouver, Canada* (pp. 1355−1358).

Baskerville, G. L. (1972). Use of logarithmic regression in the estimation of plant biomass. *Canadian Journal of Forest Research*, *1*, 49−53.

Belsley, D. A. (1990). *Conditioning diagnostics.* : John Willy & Sons.

Boegh, E., Broge, H. S. N., Hasager, C. B., Jensen, N. O., Schelde, K., & Thomsen, A. (2002). Airborne multispectral data for quantifying leaf area index, nitrogen concentration, and photosynthetic efficiency in agriculture. *Remote Sensing of Environment*, *81*, 179−193.

Bortolot, Z. J., & Wynne, R. H. (2005). Estimating forest biomass using small footprint LiDAR data: An individual tree-based approach that incorporates training data. *Journal of Photogrammetry and Remote Sensing*, *59*, 342−360.

Boyd, D. S., & Danson, F. M. (2005). Satellite remote sensing of forest resources: Three decades of research development. *Progress in Physical Geography*, *29*, 1−26.

Boyd, D. S., Foody, G. M., & Curran, P. J. (1999). The relationship between the biomass of Cameroonian tropical forests and radiation reflected in middle infrared wavelengths (3.0–5.0 μm). *International Journal of Remote Sensing*, *20*, 1017−1023.

Brown, S. (1993). Tropical forest and the global carbon cycle: The need for sustainable landuse patterns. *Agriculture, Ecosystems & Environment*, *46*, 31−44.

Brown, S., Gillespie, A. J. R., & Lugo, A. E. (1989). Biomass estimation methods for tropical forests with applications to forest inventory data. *Forest Science*, *35*, 881−902.

Calvao, T., & Palmeirim, J. M. (2004). Mapping Mediterranean scrub with satellite imagery: Biomass estimation and spectral behaviour. *International Journal of Remote Sensing*, *25*, 3113−3126.

Castel, T., Guerra, F., Caraglio, Y., & Houllier, F. (2002). Retrieval biomass of a large Venezuelan pine plantation using JERS-1 SAR data. Analysis of forest structure impact on radar signature. *Remote Sensing of Environment*, *79*, 30−41.

Champion, I., Dubois-Fernandez, P., Guyon, D., & Cottrel, M. (2008). Radar image texture as a function of forest stand age. *International Journal of Remote Sensing*, *29*, 1795−1800.

Chen, J. M. (1996). Evaluation of vegetation indices and a modified simple ratio for boreal applications. *Canadian Journal of Remote Sensing*, *22*, 229−242.

Chen, D., Stow, D. A., & Gong, P. (2004). Examining the effect of spatial resolution and texture window size on classification accuracy: An urban environment case. *International Journal of Remote Sensing*, *25*, 2177−2192.

Clevers, J. G. P. W. (1988). The derivation of a simplified reflectance model for the estimation of leaf area index. *Remote Sensing of Environment*, *25*, 53−69.

Cohen, W. B., & Spies, T. A. (1992). Estimating structural attributes of Douglas-fir/western hemlock forest stands from Landsat and SPOT imagery. *Remote Sensing of Environment*, *41*, 1−17.

Crippen, R. E. (1990). Calculating the vegetation index faster. *Remote Sensing of Environment*, *34*, 71−73.

Crow, T. R. (1978). Biomass and production in three contiguous forests in northern Wisconsin. *Ecology*, *59*, 265−273.

Curran, P. (1983). Estimating green LAI from multispectral aerial photography. *Photogrammetric Engineering and Remote Sensing*, *49*, 1709−1720.

Curran, P. J. (1988). The semi-variogram in remote sensing: an introduction. *Remote Sensing of Environment*, *3*, 493−507.

Curtis, P. S. (2008). Estimating Aboveground Carbon in Live and Standing Dead Trees. In C. M. Hoover (Ed.), *Field Measurement for Forest Carbon Monitoring* (pp. 39−44). Springer Science + Business Media B.V.

Deering, D. W., Rose, J. W., Jr., Mass, R. H., & Schell, J. A. (1975). Measuring Forage Production of Grazing Units from LANDSAT MSS Data. *Proceedings of the 10th International Symposium on Remote Sensing of Environment* (pp. 1169−1178).

Dekker, R. J. (2003). Texture analysis and classification of ERS SAR image for Map updating of urban areas in the Netherlands. *IEEE Transactions on Geoscience and Remote Sensing*, *41*, 1950−1958.

Dell'Acqua, F., & Gamba, P. (2003). Texture-based characterization of urban environments on satellite SAR images. *IEEE Transactions on Geoscience and Remote Sensing*, *41*, 153−159.

Dobson, M. C., Ulaby, F. T., Le Toan, T., Beaudoin, A., Kasischke Kasischke, E. S., & Christensen, N. C. (1992). Dependence of radar backscatter on conifer forest biomass. *IEEE Transactions on Geoscience and Remote Sensing*, *30*, 412−415.

Douglas, C. M., Peck, E. A., & Vining, G. G. (2006). *Introduction to linear regression analysis* (pp. 323−368). (Fourth edition). New Jersey: Wiley & Sons publication.

Elvidge, C. D., & Chen, Z. (1995). Comparison of broad-band and narrow band red and near infrared vegetation indices. *Remote Sensing of Environment*, *54*, 38−48.

Fassnacht, K. S., Gower, S. T., MacKenzie, M. D., Nordheim, E. V., & Lillesand, T. M. (1997). Estimating the leaf area index of North Central Wisconsin Forests USING the Landsat thematic mapper. *Remote Sensing of Environment*, *61*, 229−245.

Foody, G. M., Boyd, D. S., & Cutler, M. E. J. (2003). Predictive relations of tropical forest biomass from Landsat TM data and their transferability between regions. *Remote Sensing of Environment*, *85*, 463−474.

Foody, G. M., Cutler, M. E., McMorow, J., Dieter, P., Tangki, H., Boyd, D. S., & Douglas, I. (2001). Mapping the biomass of Bornean tropical rain forest from remotely sensed data. *Global Ecology and Biogeography*, *10*, 379−387.

Foody, G. M., Green, R. M., Curran, P. J., Lucas, R. M., Honzak, M., & Do Amaral, I. (1997). Observations on the relationship between SIR-C radar backscatter and the biomass of regenerating tropical forests. *International Journal of Remote Sensing*, *18*, 687−694.

Franklin, S. E. (2001). *Remote sensing for sustainable forest management.* : LEWIS Publication.

Franklin, S. E., Hall, R. J., Moskal, L. M., Maudie, A. J., & Lavigne, M. B. (2000). Incorporating texture into classification of forest species composition from airborne multispectral images. *International Journal of Remote Sensing*, *21*, 61−79.

Franklin, S. E., Wulder, M. A., & Lavigne, M. B. (1996). Automated derivation of geographic window sizes for remote sensing digital image texture analysis. *Computers and Geosciences*, *22*, 665−673.

Fuchs, H., Magdon, P., Kleinn, C., & Flessa, H. (2009). Estimating aboveground carbon in a catchment of the Siberian forest tundra: Combining satellite imagery and field inventory. *Remote Sensing of Environment*, *113*, 518−531.

Gibson, P. J., & Power, C. H. (2000). *Introductory Remote Sensing: Digital Image Processing and Applications.* London: Routledge.

Haralick, R. M., Shanmugam, K., & Dinstein, I. (1973). Texture features for image classification. *IEEE Transactions on Systems, Man, and Cybernetics*, *3*, 610−621.

Hay, G. J., Niemann, K. O., & McLean, G. F. (1996). An object-specific image texture analysis of H-resolution forest imagery. *Remote Sensing of Environment*, *55*, 108−122.

He, D. C., & Wang, L. (1991). Texture features based on texture spectrum. *Pattern Recognition*, *24*, 391−399.

Hudak, A. T., Lefsky, M. A., Cohen, W. B., & Berterretche, M. (2002). Integration of lidar and Landsat ETM + data for estimating and mapping forest canopy height. *Remote Sensing of Environment*, *82*, 397−416.

Hudak, A. T., & Wessman, C. A. (1998). Textural analysis of historical aerial photography to characterize woody plant encroachment in South African Savanna — II. Real digital images. *Remote Sensing of Environment*, *66*, 317−330.

Huete, A. R., Jackson, R. D., & Post, D. F. (1985). Spectral response of a plant canopy with different soil backgrounds. *Remote Sensing of Environment*, *17*, 37−53.

Huete, A. R. (1988). A Soil Adjusted Vegetation Index (SAVI). *Remote Sensing of Environment*, *25*, 295−309.

Hyde, P., Dubayah, R., Walker, W., Blair, J. B., Hofton, M., & Hunsaker, C. (2006). Mapping forest structure for wildlife habitat analysis using multi-sensor (LiDAR, SAR/InSAR, ETM+, Quickbird) synergy. *Remote Sensing of Environment*, *102*, 63−73.

Hyde, P., Nelson, R., Kimes, D., & Levine, E. (2007). Exploring LiDAR–RaDAR synergy—Predicting aboveground biomass in a southwestern ponderosa pine forest using LiDAR, SAR and InSAR. *Remote Sensing of Environment*, *106*, 28−38.

Jackson, R. D., & Huete, A. R. (1991). Interpreting vegetation indices. *Preventive Veterinary Medicine*, *11*, 185−200.

Jensen, J. R. (2000). *Remote sensing of the environment: An earth resource perspective.* Upper Saddle River, New Jersey: Prentice-Hall Inc.

Karnieli, A., Kaufman, Y. J., Remer, L., & Wald, A. (2001). AFRI — Aerosol free vegetation index. *Remote Sensing of Environment*, *77*, 10−21.

Kaufman, Y. J., & Tanre, D. (1992). Atmospherically resistant vegetation index (ARVI) for EOS-MODIS. *IEEE Transaction on Geoscience and Remote Sensing*, *30*, 261−270.

Ketterings, Q. M., Coe, R., van Noordwijk, M., Ambagau, Y., & Palm, C. A. (2001). Reducing uncertainty in the use of allometric biomass equations for predicting above-ground tree biomass in mixed secondary forests. *Forest Ecology and Management*, *146*, 199−209.

Kimes, D. S., Nelson, R. F., Manry, M. T., & Fung, A. K. (1998). Attributes of neural networks for extracting continuous vegetation variables from optical and radar measurements. *International Journal of Remote Sensing*, *19*, 2639−2663.

Kriegler, F. J., Malila, W. A., Nalepka, R. F., & Richardson, W. (1969). Preprocessing transformations and their effect on multispectral recognition. *Proceedings of the sixth International Symposium on Remote Sensing of Environment* (pp. 97−131). Ann Arbor, MI: University of Michigan.

Kuplich, T. M., Curran, P. J., & Atkinson, P. M. (2005). Relating SAR image texture to the biomass of regenerating tropical forest. *International Journal of Remote Sensing*, *26*, 4829−4854.

Kutner, M. H., Nachtsheim, C. J., Neter, J., & Li, W. (2005). *Applied linear statistical models.* McGraw-Hill/Irwin publication.

Laine, A., & Fan, J. (1993). Texture classification by wavelet packet signatures. *IEEE Transactions on Pattern Analysis and Machine Intelligence*, *15*, 1186−1191.

Le Toan, T., Beaudoin, A., Riom, J., & Guyon, D. (1992). Relating forest biomass to SAR data. *IEEE Transactions on Geoscience and Remote Sensing*, *30*, 403−411.

Lu, D. (2005). Aboveground biomass estimation using Landsat TM data in the Brazilian Amazon. *International Journal of Remote Sensing*, *26*, 2509−2525.

Lu, D. (2006). The potential and challenge of remote sensing-based biomass estimation. *International Journal of Remote Sensing*, *27*, 1297−1328.

Luckman, A., Frery, A. C., Yanasse, C. C. F., & Groom, G. B. (1997). Texture in airborne SAR imagery of tropical forest and its relationship to forest regeneration stage. *International Journal of Remote Sensing*, *18*, 1333−1349.

Luettgen, M. R., Karl, W. C., Willsky, A. S., & Tenney, R. R. (1993). Multiscale representations of Markov random fields. *IEEE Transactions on Signal Processing*, *41*, 3377−3396.

Marceau, D. J., Howarth, P. J., Dubois, J. M., & Gratton, D. J. (1990). Evaluation of the graylevel co-occurrence matrix method for land cover classification using SPOT imagery. *IEEE Transactions on Geoscience and Remote Sensing*, *28*, 513−517.

Mather, P. M. (1999). *Computer processing of remotely sensed images* (2nd end.). Chichester: Wiley.

Mitchard, E. T. A., Saatchi, S. S., Woodhouse, I. H., Nangendo, G., Ribeiro, N. S., Williams, M., Ryan, C. M., Lewis, S. L., Feldpausch, T. R., & Meir, P. (2009). Using satellite radar backscatter to predict above-ground woody biomass: A consistent relationship across four different African landscapes. *Geophysical Research Letters*, *36*, L23401, doi:10.1029/2009GL040692

Montagu, K. D., Duttmer, K., Barton, C. V. M., & Cowie, A. L. (2005). Developing general allometric relationships for regional estimates of carbon sequestration—An example using *Eucalyptus pilularis* from seven contrasting sites. *Forest Ecology and Management*, *204*, 113−127.

Moran, E. F., Brondizio, E., Mausel, P., & Wu, Y. (1994). Integrating Amazonian vegetation, land-use, and satellite data: Attention to differential patterns and rates of secondary succession can inform future policies. *Bioscience*, *44*, 329−338.

Muukkonen, P., & Heiskanen, J. (2007). Biomass estimation over a large area based on standwise forest inventory data and ASTER and MODIS satellite data: A possibility to verify carbon inventories. *Remote Sensing of Environment*, *107*, 617−622.

Nelson, R. F., Kimes, D. S., Salas, W. A., & Routhier, M. (2000). Secondary forest age and tropical forest biomass estimation using Thematic Mapper imagery. *Bioscience*, *50*, 419−431.

Nelson, R., Krabill, W., & Tonelli, J. (1988). Estimating forest biomass and volume using airborne laser data. *Remote Sensing of Environment*, *24*, 247−267.

Overman, J. P. M., Witte, H. J. L., & Saldarriaga, J. G. (1994). Evaluation of regression models for above-ground biomass determination in Amazon rainforest. *Journal of Tropical Ecology*, *10*, 207−218.

Parresol, B. R. (1999). Assessing Tree and Stand Biomass: A Review with Examples and Critical Comparisons. *Forest Science*, *45*, 573−593.

Patenaude, G., Hill, R. A., Milne, R., Gaveaud, D. L. A., Briggs, B. B. J., & Dawson, T. P. (2004). Quantifying forest above ground carbon content using LiDAR remote sensing. *Remote Sensing of Environment*, *93*, 368−380.

PCI Geomatica (2007). *PCI Geomatica OrthoEngine 10.1 User Guide, 50 West Wilmot Street, Richmond Hill, Ontario, Canada.*

Pearson, R. L., & Miller, L. D. (1972). Remote mapping of standing crop biomass for estimation of the productivity of the short-grass Prairie, Pawnee National Grasslands, Colorado. *Proc. of the 8th International Symposium on Remote Sensing of Environment* (pp. 1357−1381). Ann Arbor, MI: ERIM.

Perry, C. R., & Lautenschlager, L. F. (1984). Functional equivalence of spectral vegetation indices. *Remote Sensing of Environment*, *14*, 169−182.

Peterson, D. L., Spanner, M. A., Running, S. W., & Teuber, K. B. (1987). Relationship of Thematic Mapper simulator data to leaf area index of temperate coniferous forests. *Remote Sensing of Environment*, *22*, 323−341.

Pinty, B., & Verstraete, M. M. (1991). Extracting information on surface properties from bidirectional reflectance measurement. *Journal of Geophysical Research*, *96*, 2865−2874.

Podest, E., & Saatchi, S. (2002). Application of multiscale texture in classifying JERS-1 radar data over tropical vegetation. *International Journal of Remote Sensing*, *23*, 1487−1506.

Qi, J., Chehbouni, A., Huete, A. R., Kerr, Y. H., & Sorooshian, S. (1994). A Modified Soil Adjusted Vegetation Index. *Remote Sensing of Environment*, *48*, 119−126.

Rahman, M. M., Csaplovics, E., & Koch, B. (2005). An efficient regression strategy for extracting forest biomass information from satellite sensor data. *International Journal of Remote Sensing*, *26*, 1511−1519.

Richardson, A. J., & Wiegand, C. L. (1977). Distinquishing vegetation from soil background information. *Photogrammetric Engineering and Remote Sensing*, *43*, 1541−1552.

Rosenqvist, Å., Milne, A., Lucas, R., Imhoff, M., & Dobson, C. (2003). A review of remote sensing technology in support of the Kyoto protocol. *Environmental Science & Policy*, *6*, 441−455.

Rouse, J. W., Haas, R. H., Schell, J. A., Deering, D. W., & Harlan, J. C. (1974). Monitoring the vernal advancement of retrogradation of natural vegetation. *Type III, Final report*. Greenbelt, Maryland, USA: NASA/GSFC.

Ryherd, S., & Woodcock, C. E. (1996). Combining spectral and texture data in the segmentation of remotely sensed images. *Photogrammetric Engineering and Remote Sensing*, *62*, 181−194.

Sader, S. A., Waide, R. B., Lawrence, W. T., & Joyce, A. T. (1989). Tropical forest biomass and successional age class relationships to a vegetation index derived from Landsat TM data. *Remote Sensing of Environment*, *28*, 143−156.

Salvador, R., & Pons, X. (1998). On the reliability of Landsat TM for estimating forest variables by regression techniques: A methodological analysis. *IEEE Transactions on Geoscience and Remote Sensing*, *36*, 1888−1897.

Santos, J. R., Freitas, C. C., Araujo, L. S., Dutra, L. V., Mura, J. C., Gama, F. F., Soler, L. S., & Sant'Anna, S. J. S. (2003). Airborne P-band SAR applied to the aboveground biomass studies in the Brazilian tropical rainforest. *Remote Sensing of Environment*, *87*, 482−493.

Schowengerdt, R. A. (1983). *Techniques for image processing and classification in remote sensing.* New York: Academic Press.

Skole, D. L., Chomentowski, W. H., Salas, W. A., & Nobre, A. D. (1994). Physical and human dimensions of deforestation in Amazonia. *Bioscience*, *44*, 314−322.

Steininger, M. K. (2000). Satellite estimation of tropical secondary forest above-ground biomass: Data from Brazil and Bolivia. *International Journal of Remote Sensing*, *21*, 1139−1157.

St-Onge, B. A., & Cavayas, F. (1997). Automated forest structure from high resolution imagery based on directional semivariogram estimates. *Remote Sensing of Environment*, *61*, 82−95.

Thenkabail, P. S., Smith, R. B., & De Pauw, E. (2000). Hyperspectral vegetation indices and their relationships with agricultural crop characteristics. *Remote Sensing of Environment*, *71*, 158−182.

Thenkabail, P. S., Stucky, N., Griscom, B. W., Ashton, M. S., Diels, J., Meer, B. V. D., & Enclona, E. (2004). Biomass estimations and carbon stock calculations in the oil palm plantations of African derived savannas using IKONOS data. *International Journal of Remote Sensing*, *25*, 5447−5472.

Thiam, A. K. (1997). Geographic Information System and Remote Sensing Methods for Assessing and Monitoring Land Degradation in the Shale: The Case of Southern Mauritania, Doctoral Dissertation, Darks University.

Tucker, C. J. (1979). Red and photographic infrared linear combinations for monitoring vegetation. *Remote Sensing of Environment*, *8*, 127−150.

Tuominen, S., & Pekkarinen, A. (2005). Performance of different spectral and textural aerial photograph features in multi-source forest inventory. *Remote Sensing of Environment*, *94*, 256−268.

Ulaby, F. T., Kouyate, F., Brisco, B., & Williams, T. H. L. (1986). Textural information in SAR images. *IEEE Transactions on Geoscience and Remote Sensing*, *24*, 235−240.

Unser, M. (1986). Sum and difference histogram for texture classification. *IEEE Transactions on Pattern Analysis and Machine Intelligence*, *PAMI-8*, 118−125.

Unser, M. (1995). Texture classification and segmentation using wavelet frames. *IEEE Transactions on Image Processing*, *4*, 1549−1560.

Wolter, P. T., Townsend, P. A., & Sturtevant, B. R. (2009). Estimation of forest structural parameters using 5 and 10 meter SPOT-5 satellite data. *Remote Sensing of Environment*, *113*, 2019−2036.

Woodcock, C. E., Strahler, A. H., & Jupp, D. L. B. (1988). The use of variograms in remote sensing: II. Real digital images. *Remote Sensing of Environment*, *25*, 349−379.

Wulder, M. A., Franklin, S. E., & Lavigne, M. B. (1996). High spatial resolution optical image texture for improved estimation of forest stand leaf area index. *Canadian Journal of Remote Sensing*, *22*, 441−449.

Zheng, D., Rademacher, J., Chen, J., Crow, T., Bresee, M., Le Moine, J., & Ryu, S. (2004). Estimating aboveground biomass using Landsat 7 ETM + data across a Biomass estimation 1327 managed landscape in northern Wisconsin, USA. *Remote Sensing of Environment*, *93*, 402−411.